

Supporting Information

A Tale of Seemingly “Identical” Silicon Quantum
Dot Families: Structural Insight into Silicon
Quantum Dot Photoluminescence.

*Alyxandra N. Thiessen^a, Lijuan Zhang^b, Anton O. Oliynyk^c, Haoyang Yu^a, Kevin M. O'Connor^a,
Alkiviathes Meldrum^b, and Jonathan G. C. Veinot^{a*}*

^a *Department of Chemistry, University of Alberta, Edmonton, Alberta T6G 2G2, Canada*

^b *Department of Physics, University of Alberta, Edmonton, Alberta T6G 2E1, Canada*

^c *Manhattan College, Riverdale, New York, United States, 10471*

* Corresponding author's email: jveinot@ualberta.ca

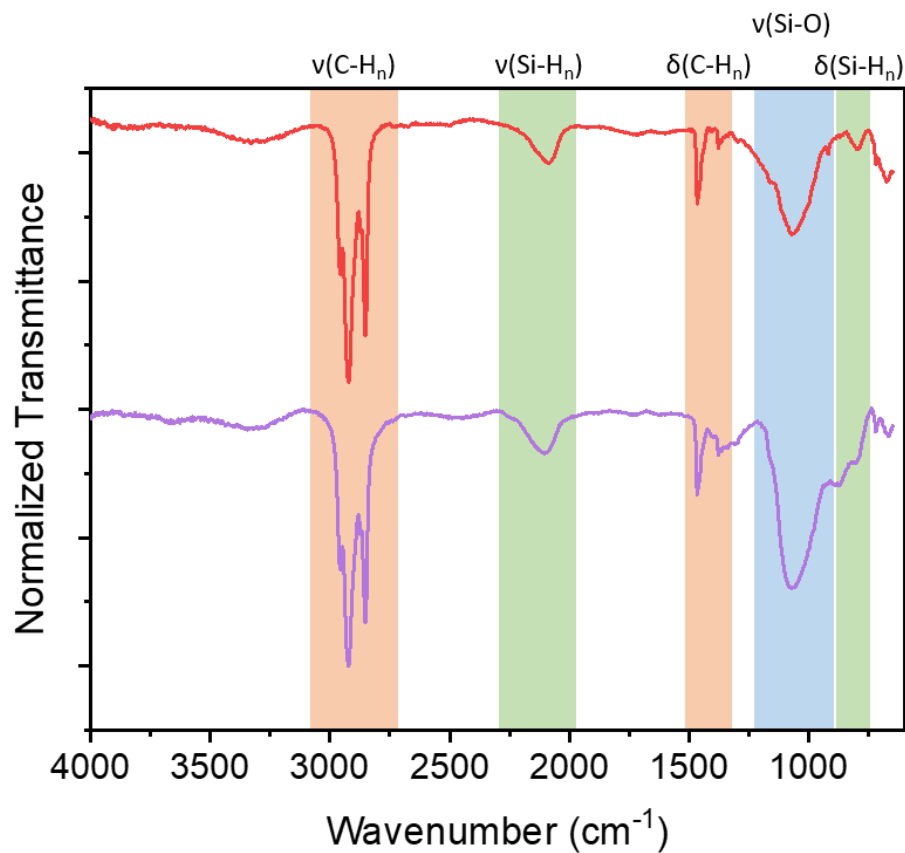


Figure S1: FTIR of 1200-SiQDs (red) and 1300-SiQDs (purple).

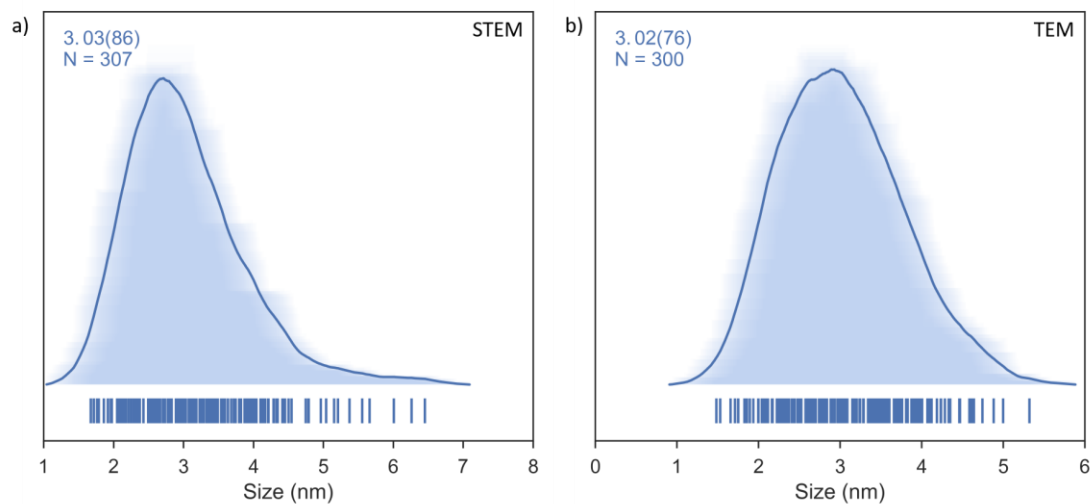


Figure S2: Average-shifted histograms showing size distributions derived from a) STEM and b) TEM images collected on identical SiNPs, using a JEOL JEM-ARM200CF S/TEM electron microscope.

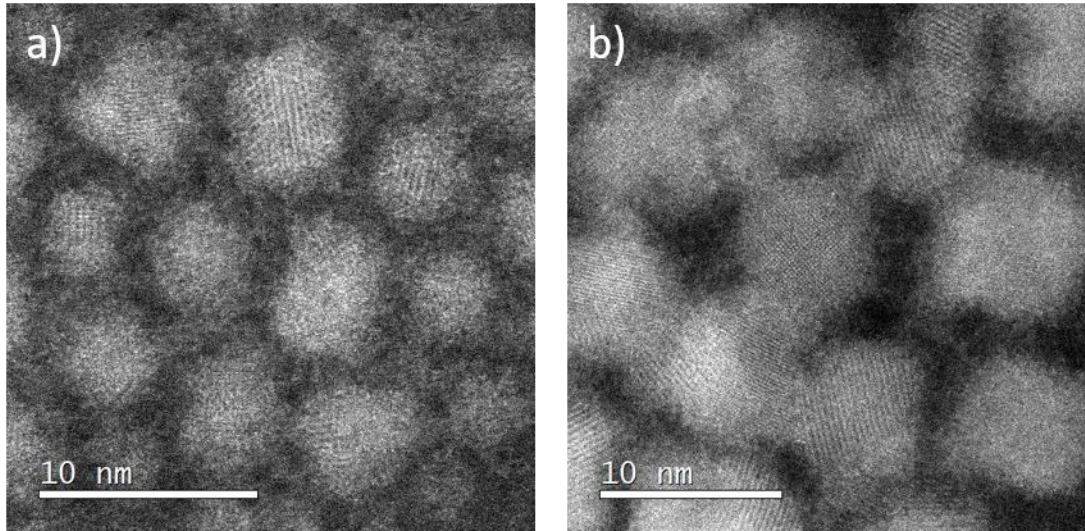


Figure S3: High annular angle dark field STEM images of a) 1200-SiQDs and b) 1300-SiQDs.

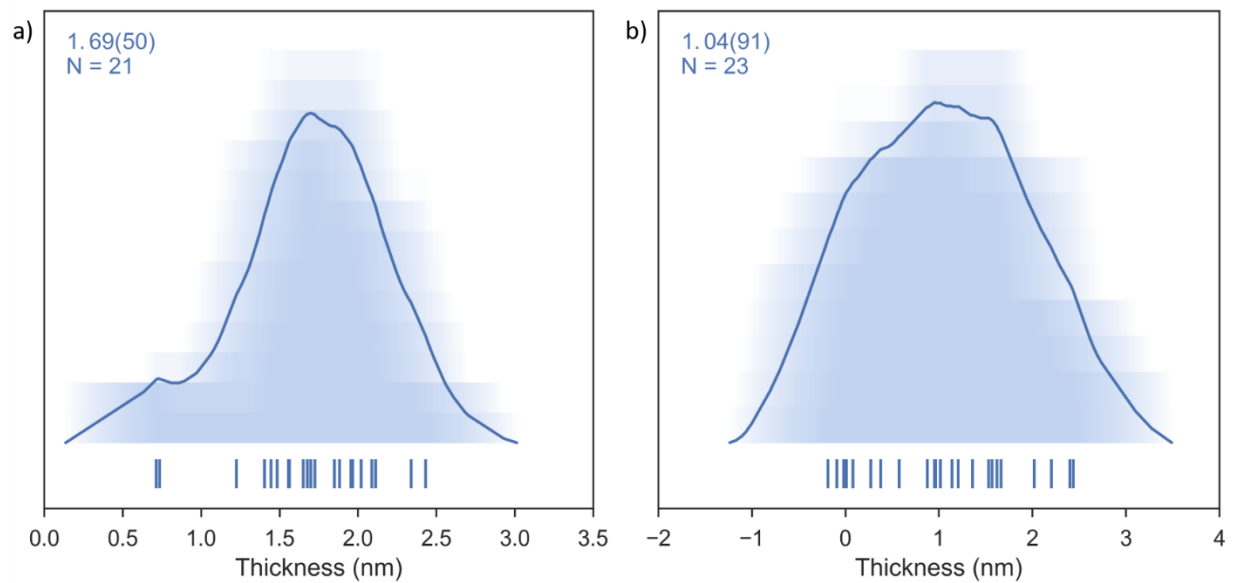


Figure S4: Histograms showing the STEM determined non-crystalline shell thicknesses for a) 1200-SiQDs and b) 1300-SiQDs. Experimental data are represented by the blue bars below the x-axis. The density of these bars indicates the frequency. The line in the plot was determined using a fitting routine described in Ref #75 that is designed to minimize binning bias.

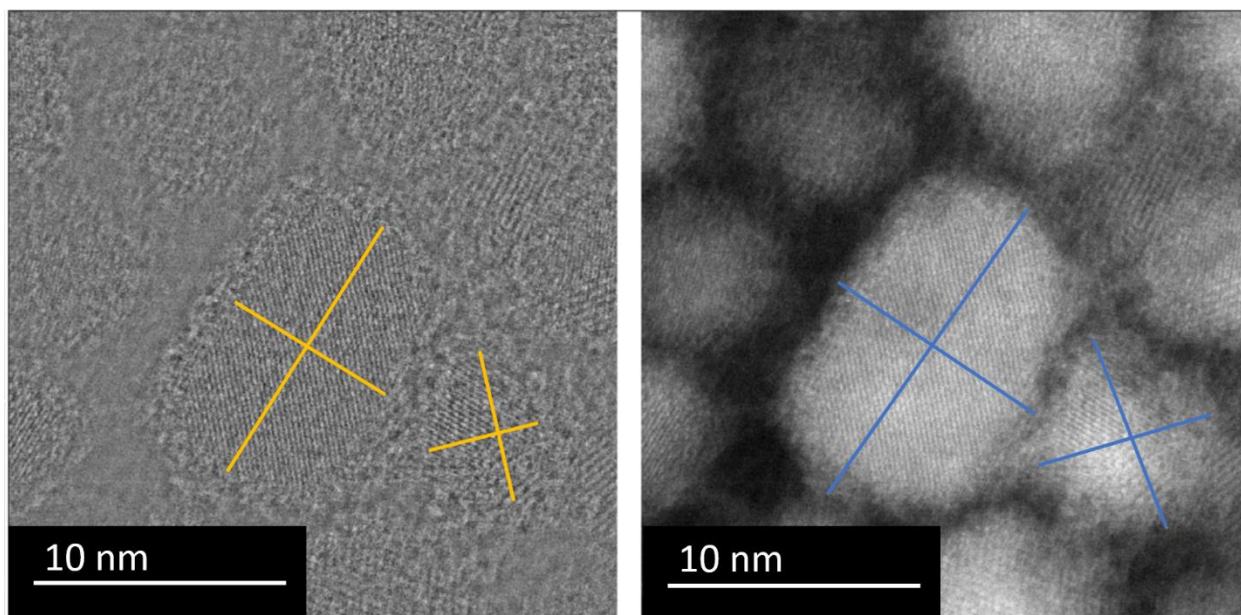


Figure S5: a) Trend subtracted STEM image highlighting lattice fringes of sample. b) Original HAADF STEM image showing full size of SiNCs. (Note: Colored lines illustrate particle measurement method.)

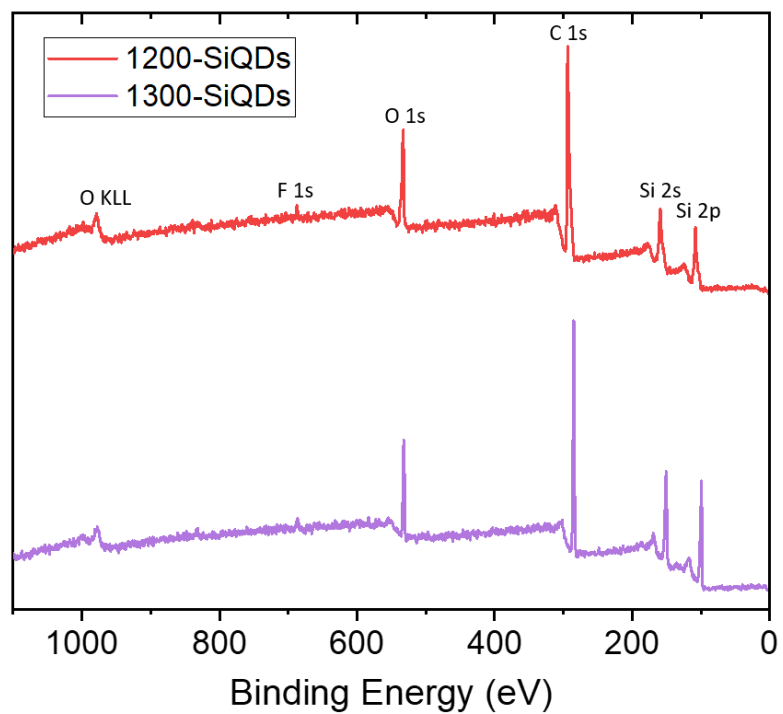


Figure S6: Survey XPS scan for a) 1200-SiQDs and b) 1300-SiQDs, showing the presence of only Si, C, O and F.

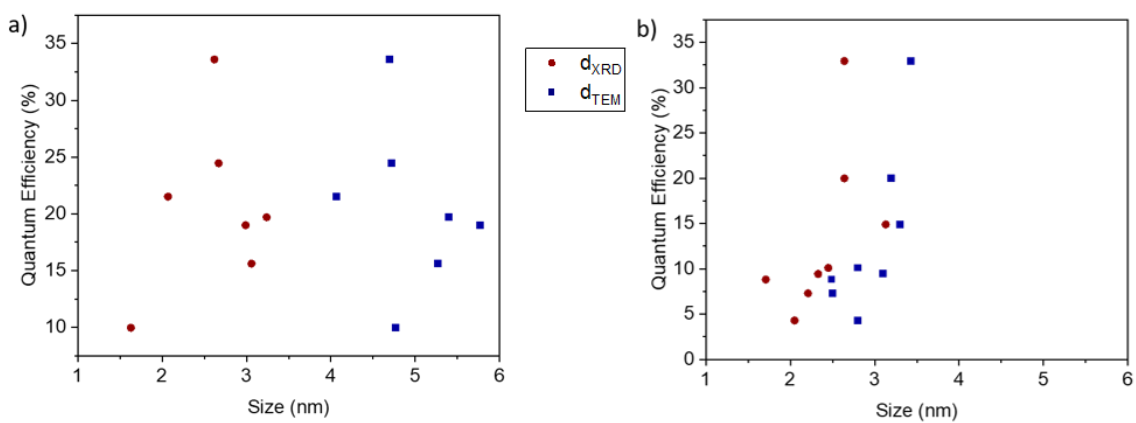


Figure S7: A comparison of the relationship between quantum efficiency with d_{TEM} (blue squares) and d_{XRD} (red circles) for SiQDs with a thick amorphous layer (>2 nm; a) and a thin amorphous layer (<0.8 nm; b).

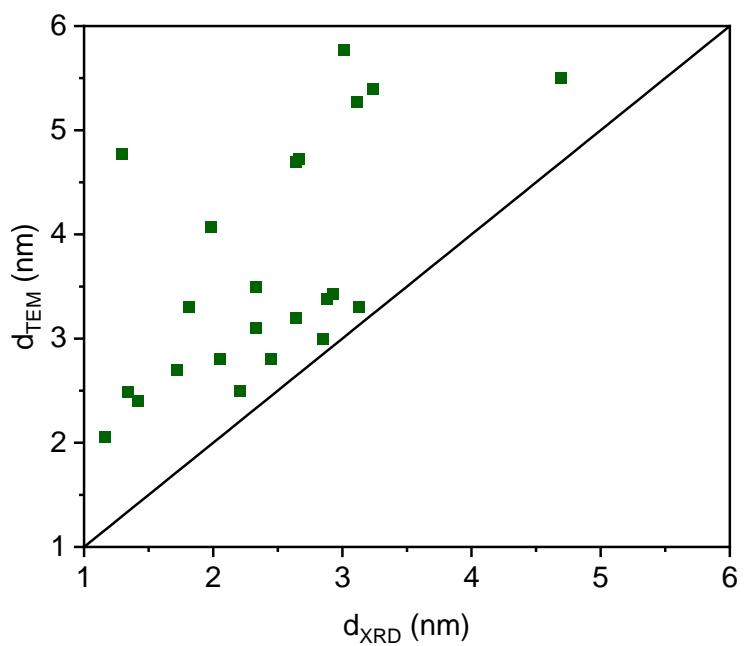


Figure S8: Plot showing d_{TEM} vs. d_{XRD} , where the line is $d_{TEM} = d_{XRD}$.

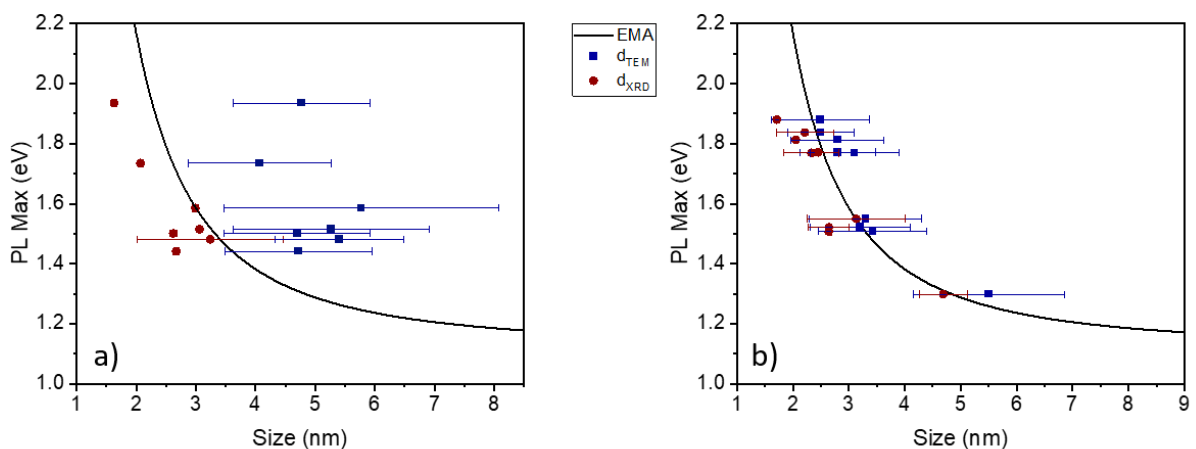


Figure S9: A comparison of the relationship between PL energy with d_{TEM} (blue squares; standard deviation shown in blue error bars) and d_{XRD} (red circles; fit errors shown in red error bars) for SiQDs with a thick amorphous layer (>2 nm; a) and a thin amorphous layer (<0.8 nm; b). The solid black line in a) and b) represents the EMA as predicted using $E_g(r) = 1.12 + 4.19/r^2$.

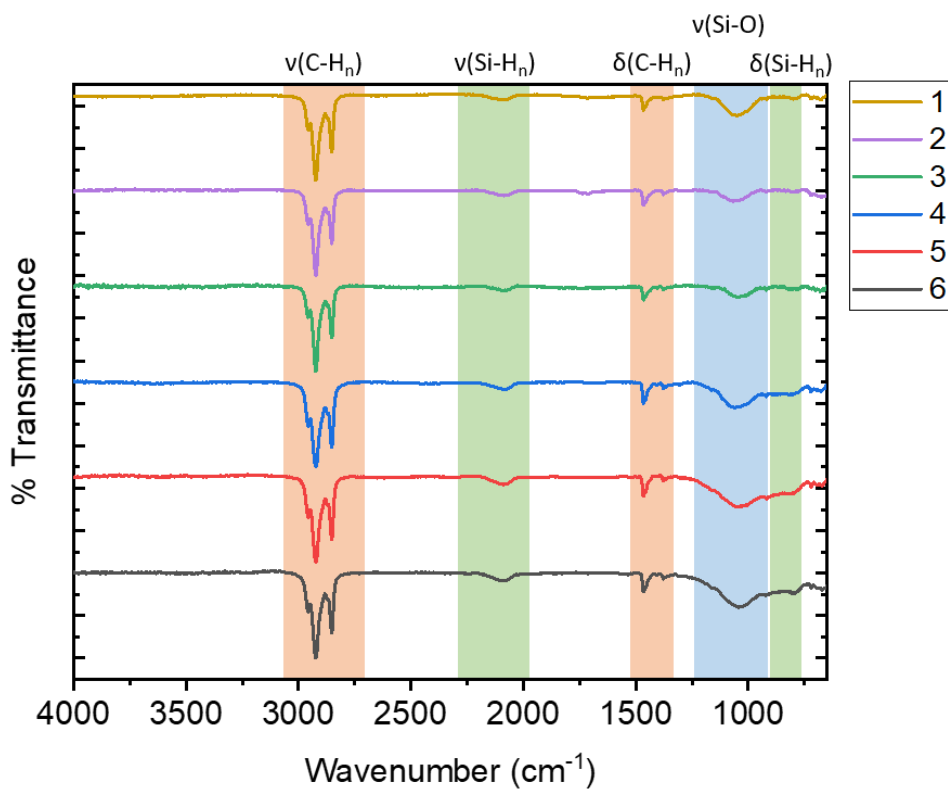


Figure S10: Representative FTIR data showing samples 1 (gold), 2 (purple), 3 (green), 4 (blue), 5 (red), 6 (black). Sample numbers refer to numbers in Table S1.

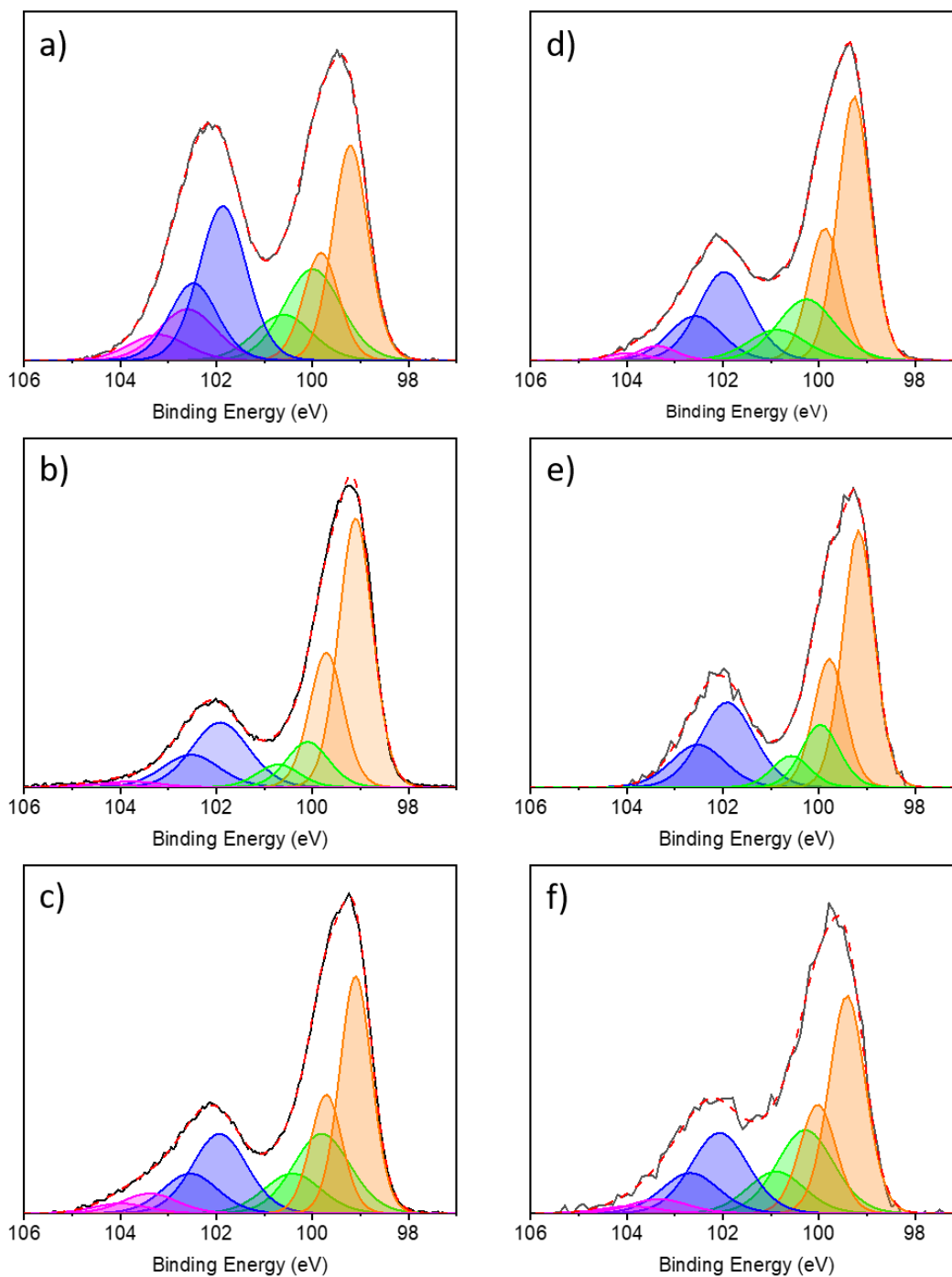


Figure S11: Representative Si 2p XPS data for samples a) 1, b) 2, c) 3, d) 4, e) 5, and f) 6. The oranges peaks represent Si (0); green, Si(I); blue, Si(III); and magenta, Si(IV). The black solid line shows the experimental data and the red dashed line represents the fitting envelope. Sample numbers refer to numbers in Table S1.

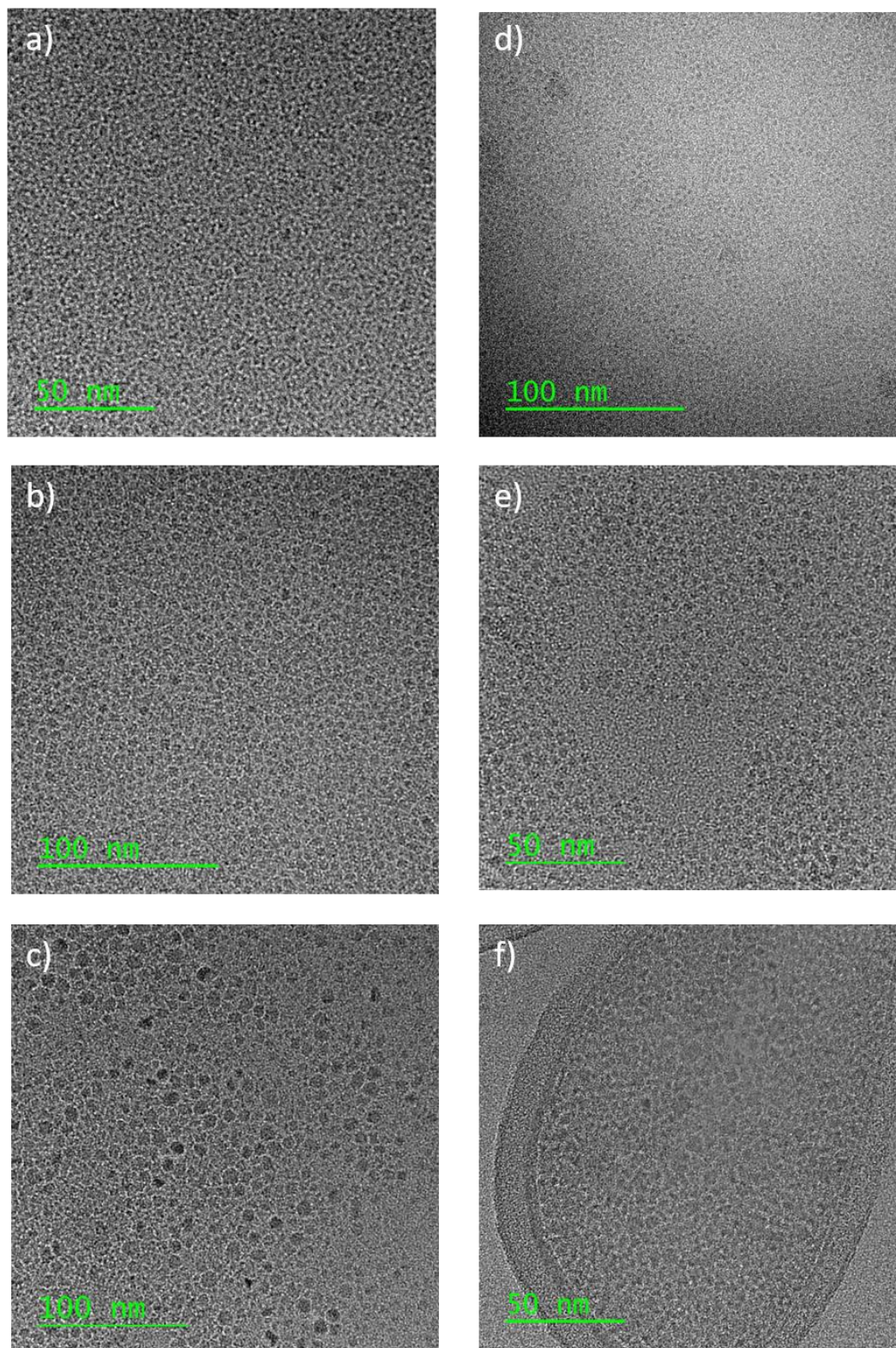


Figure S12: Representative bright field TEM a) 1, b) 2, c) 3, d) 4, e) 5, and f) 6. Sample numbers refer to numbers in Table S1.

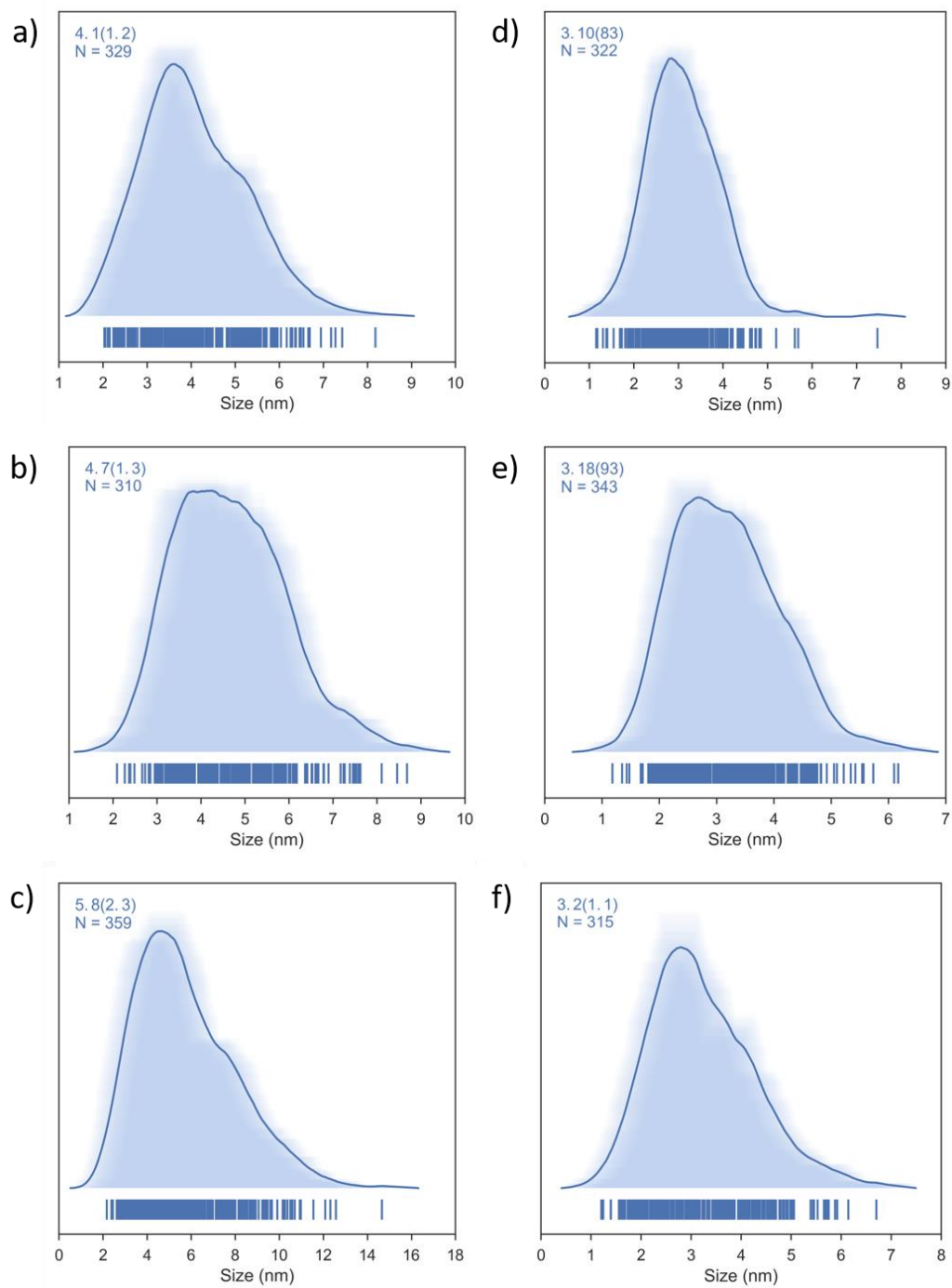


Figure S13: Average shifted histograms for SiNCs counted from TEM/STEM images for samples a) 1, b) 2, c) 3, d) 4, e) 5, and f) 6. Sample numbers refer to numbers in Table S1. The line in the plot was determined using a fitting routine described in Ref #75 that is designed to minimize binning bias.

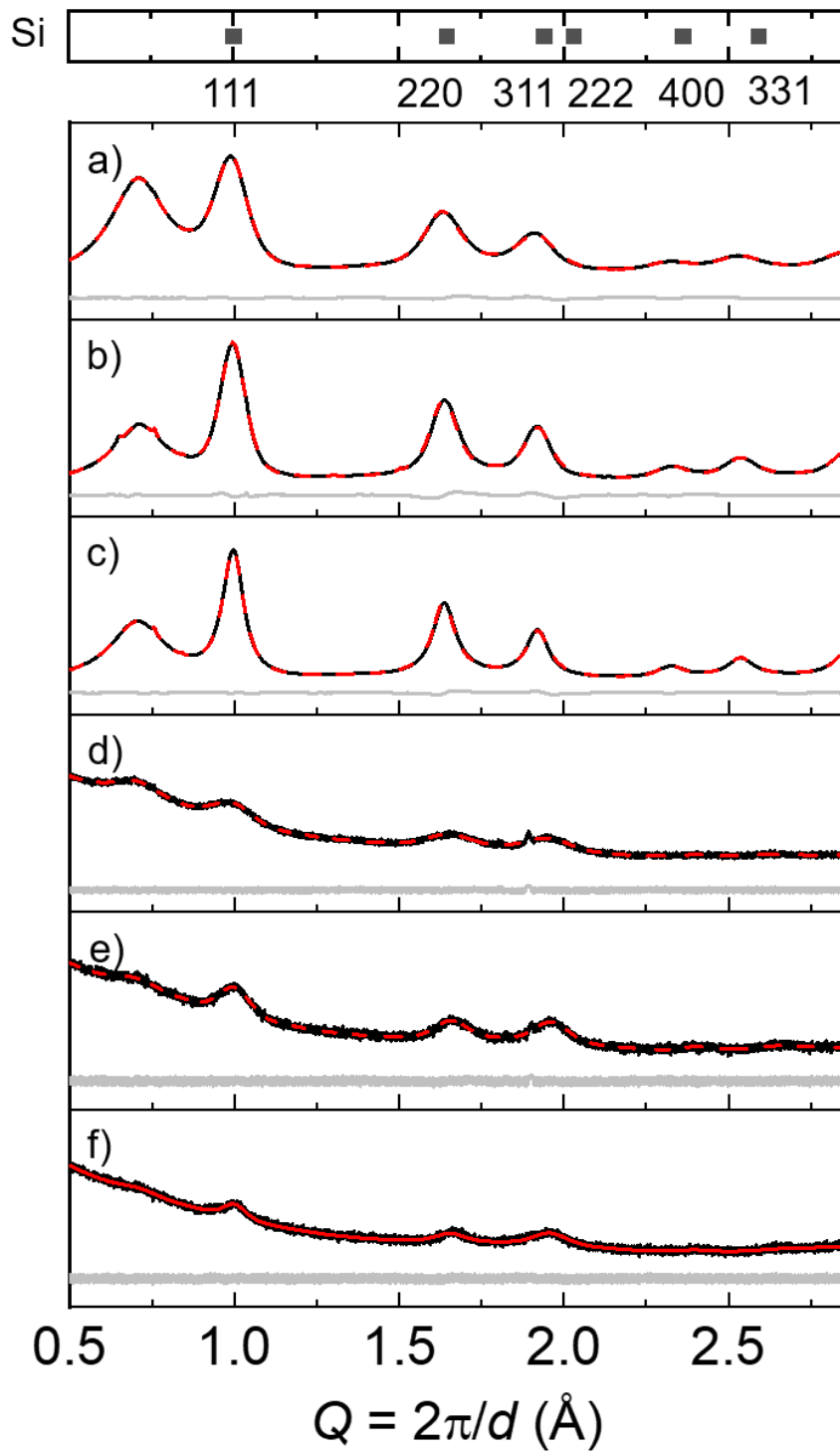


Figure S14: X-ray diffraction powder patterns for samples a) 1, b) 2, c) 3, d) 4, e) 5, and f) 6. The black trace is the experimental data, the red is the fit and the grey is the difference. Samples a-c were collected at the Canadian Light Source synchrotron facility ($\lambda=0.6891$) and samples d-f was collected on the Rigaku Ultima with a Cu-K α source. Sample numbers refer to numbers in Table S1.

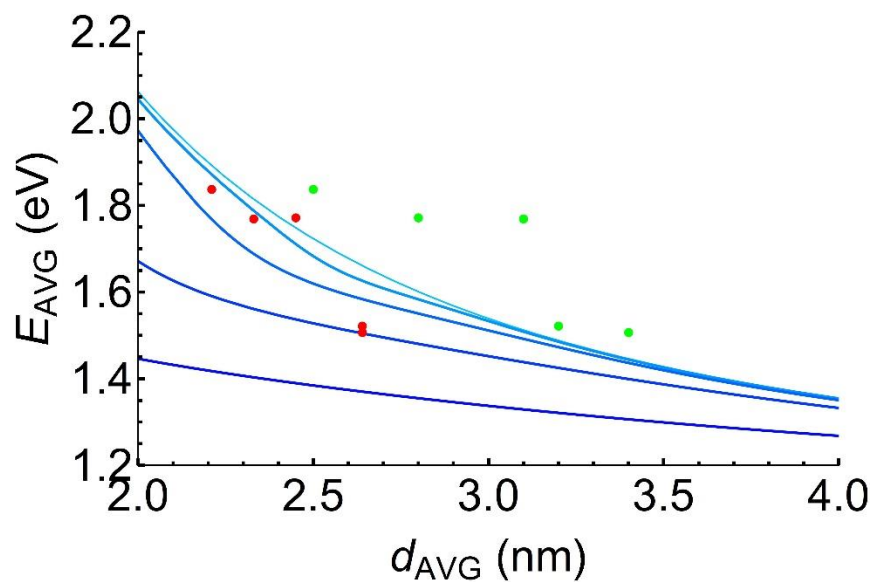


Figure S15. The XRD (red points) and TEM (green points) mean diameters as a function of the mean PL energy. The blue lines are model fits that incorporate the quantum efficiency, absorption cross sections, size distributions, and effective mass approximation using methods similar to those in Ref. Yu et al. 2017). The uppermost light blue line is the pure EMA; increasing the size distribution “pulls” the model downward mainly due to the higher QY of the larger particles (darker blue lines).

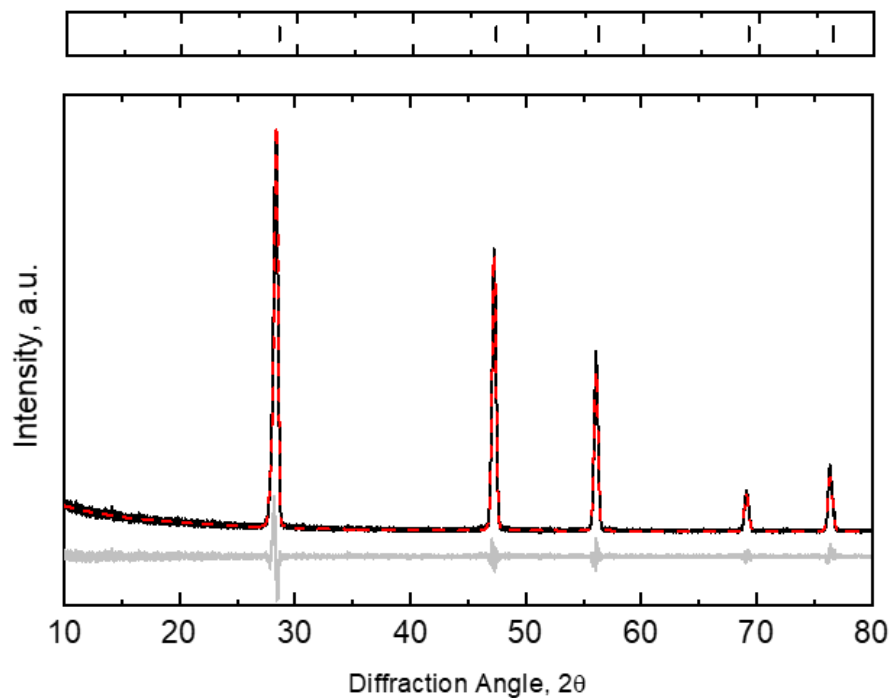


Figure S16: Fitting of Si NIST linewidth standard (640f) measured on the Rigaku Ultima IV.

Table S1: A summary of experimental parameters and results for all samples

Sample #	Anneal T ^a (°C)	Etch time ^b (min)	d _{TEM} (nm)	d _{XRD} (nm)	PL Max (nm)	Lifetime ^c (μs)	QE ^d (%)
1300-SiQD ^e	1300	240 ^g	5.5	4.69	955	546.8	N/A
1200-SiQD ^f	1200	60	5.4	3.24	837	266.6	19.7
1 ^f	1200	90	4.1	2.07	715	98.8	21.5
2 ^f	1200	60	4.7	2.62	826	190.4	33.6
3 ^f	1300	135	5.8	2.99	782	135.7	19.0
4 ^e	1200	165	3.1	2.33	701	97.0	9.4
5 ^e	1200	75	3.2	2.64	815	218.7	20
6 ^e	1300	240	3.3	3.13	800	208.1	14.9
7 ^e	1100	30	2.8	1.71	659	73.6	8.8
8 ^e	1200	60	3.4	2.64	823	172.1	33.0
9 ^e	1200	130	2.5	2.21	675	81.6	7.3
10 ^e	1200	120	2.8	2.45	700	98.5	10.1
11 ^e	1100	45	2.8	2.05	684	107.3	4.3
12 ^f	1300	210	5.3	3.06	819	159.0	15.6
13 ^f	1200	105	4.8	1.63	641	63.1	10.0
14 ^f	1200	40	4.7	2.67	860	205.7	24.5

^a Temperature used for annealing HSQ to make the composite

^b Time used for HF etching

^c Mean lifetimes were calculated as described above.

^d Quantum efficiency

^e “Thin” amorphous shell samples (Figure 5 d,f).

^f “Thick” amorphous shell samples (Figure 5 c,e).

^g 5 mL of 49% HF added halfway through etch.

Table S2: Lifetime fitting parameters for 1200-SiQDs and 1300-QDs

	<i>A</i>	<i>β</i>	<i>Dc</i>
1200-SiQDs	1.031	0.8608	0.00091
1300-SiQDs	1.024	0.8346	0.0053